34th Annual International Conference of the IEEE EMBS
San Diego, California USA, 28 August - 1 September, 2012

Combination of Amplitude and Phase Features under a Uniform Framework with EMD in EEG-based Brain-Computer Interface

Wei He, Pengfei Wei, Yi Zhou and Liping Wang

Abstract— **In a Brain-Computer Interface (BCI) system, the variations of the amplitude and the phase in EEG signal convey subjects' movement intention and underpin the differentiation of the various mental tasks. Combining these two kinds of information under a uniform feature extraction framework can better reflect the brain states and potentially contribute to BCI classification. Here the Common Spatial Pattern (CSP) and the Phase Locking Value (PLV) were used to capture the amplitude and the phase information. To integrate these two feature extraction procedures, the Empirical Mode Decomposition (EMD) is introduced in preprocessing which behaved as filter bank to optimize bands selection automatically for CSP and exactly calculate the instantaneous phase for PLV. The most discriminative features were selected from the feature pool by the sequential floating forward feature selection method (SFFS). The proposed method was applied to both public and recorded datasets (each n=4). Compared with the traditional CSP, the average increment of classification accuracy is 5.4% (2.0% for public and 8.7% for recorded datasets), which both manifests statistically significances ($p<0.05$). Moreover, we preliminarily investigate the possibility of the online realization of this method and it shows a comparable result with the offline result.**

I. Introduction

Brain-computer interface (BCI) system detects the human motor intention based on various senor modalities such as electroencephalogram (EEG) recordings and translates it as the control signal to outside devices without using nerves and muscles [1]. In a popular motor imagery (MI) based EEG BCI system, the commonly used signal pattern is the sensorimotor rhythms amplitude changes in the primary motor cortex (M1) during movement imagination, which called event related desynchronization/synchronization (ERD/ERS) [2]. Moreover, the phase coupling of oscillatory activity which represents the interaction between M1 and supplementary motor area (SMA) is also a characteristic of MI [3]. Combination of the amplitude and the phase information under a uniform feature extraction framework could better reflect brain activities and potentially facilitate the BCI classification.

Different feature extraction methods have been proposed to distinguish variant mental tasks. To detect the ERD/ERS characterized MI intention, a popular algorithm named Common Spatial Pattern (CSP) is utilized to construct spatial filters to maximize the variance between two mental tasks [4]. To quantify the phase coupling represented MI intention, phase locking value (PLV) is applied to calculate the instantaneous phase difference in a statistical means between two EEG channels in relevant frequency band [3]. Therefore, it is a straightforward idea that incorporation of these two feature extraction methods could provide reliable features and contribute to enhance classification accuracy. However, the effective of CSP relies on pre-filtering EEG signal into the specific frequency bands that mostly correlated with the MI. And the reliable PLV estimation depends on precisely extracting the instantaneous phase within a single narrow band component. In order to integrate these two methods, novel signal processing approach is required to meet the dynamic phase changes of EEG signal and adaptively optimize the specify frequency selection for individual subject.

In this paper, we employ empirical mode decomposition (EMD) [5] to satisfy these two requirements simultaneously. The EMD method could behave as filter bank [6] and the EMD decomposed intrinsic mode functions (IMFs) in a sifting process have well-behaved Hilbert transforms. In this way, the specific frequency band could be selected automatically and the instantaneous phase could be well-calculated. And then, the sequential floating forward feature selection algorithm (SFFS [7]) is used to select the most discriminative features for next step classification. Public BCI competition IV dataset I with four subjects performing left and right hand mental tasks and recorded EEG dataset from four volunteers are used to evaluate the proposed method. The architecture of the proposed method is shown in Fig. 1.

II. Proposed Methods

A. EEG Acquisition and Online Experimental Paradigm

Four naïve right-handed healthy subjects participated in the experiment. The EEG signal was sampled at 1000Hz. Forty one electrodes over M1 and SMA was selected. The experiment paradigm was that: during the beginning 2 seconds, two relaxing hands on the screen were presented to the subject, and a "Ready" cue was shown to draw the subject's attention in next 2 seconds. At second 4, a "Go" cue was appearing to instruct the subject to fulfill a hand grasping task in the virtual world. The subject was asked to control the virtual hand to catch a tennis ball by imagining hand movement in a 4 seconds period. The position of the virtual hands was determined by the power difference between two pre-selected electrodes for each subject. The online experiment paradigm was shown in Fig. 2 and the EEG data was recorded for further analysis. The recorded dataset comprised 200 trials (100 per class) in two sessions. The rest time between two sessions is 15 minutes. The trials with obvious eye movement artifacts were excluded by visualizing.

Manuscript received March 29, 2012. (Write the date on which you submitted your paper for review.)

W. He, P. Wei, Y. Zhou and L. Wang are with Shenzhen Key Lab of Neuropsychiatric Modulation, Shenzhen Institutes of Advanced Technology, Chinese Academy of Sciences, Shenzhen 518055, China (e-mail: weo.he@siat.ac.cn, yi.zhou@siat.ac.cn ,lp.wang@siat.ac.cn, corresponding author to provide phone :+8615302783650, e-mail: pf.wei @ siat.ac.cn)

The work is supported by National Basic Research Program of China (973 program: 2010CB529605) and Science and Technology Funds of Shenzhen (Key Lab Program: CXB201104220025A)

For a more reliable comparison to other public methods, a public dataset from BCI competition IV dataset I with four subjects was also used to perform the method evaluation.

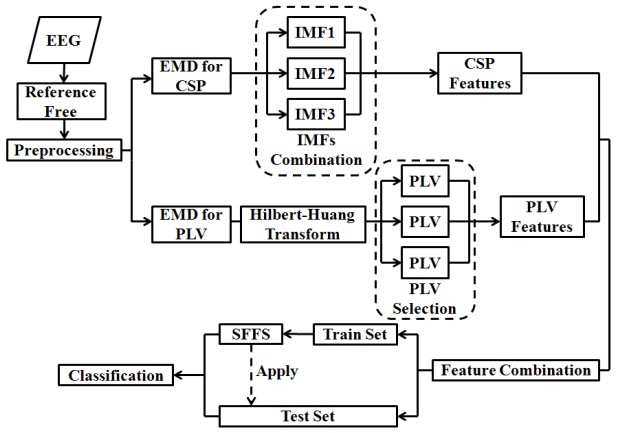

Figure 1. Architecture of the proposed method

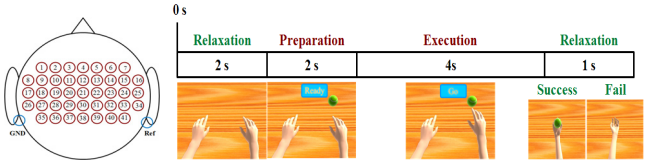

Figure 2. The electrode postions of the recorded dataset (left) and the paradiam (right) of the online experimment

B. Reference-free and Preprocessing

As the potential from the recording reference electrode could contaminate the EEG signal and distort the subsequent PLV calculation [8], we employed a method [9] to identify and remove the activity from the reference electrode. The reference potential $\hat{ref}(t)$ was estimated as:

$$\hat{ref}(t) = \mathbf{w}^T \mathbf{x}(\mathbf{t}) \quad \mathbf{w} = -\frac{\mathbf{\Phi_{xx}^{-1}}}{1^T \mathbf{\Phi_{xx}^{-1}} 1} 1 \tag{1}$$

where $\mathbf{x(t)}$ is the EEG signal. $\mathbf{\Phi_{xx}}$ is the correlation matrix of $\mathbf{x(t)}$ and 1 is a vector of ones. After that, the reference potential was subtracted and the EEG signal was filtered in 7-30Hz and 5-40Hz for CSP and PLV procedure separately.

C. EMD Algorithm

EMD method is a data-driven and self-adaptive approach that represents a signal as a sum of amplitude modulation frequency modulation components [5]. EMD decomposes a given signal into IMFs and residual that could be expressed as:

$$x(t) = \sum_{i=1}^{n} c_i(t) + r(t) \tag{2}$$

where $x(t)$ is the given signal, $c_i(t), i = 1, \ldots n$ is the decomposed IMFs and $r(t)$ is the residual. For the detailed procedure of the sifting process could see [5].

D. CSP Algorithm

The CSP method constructs spatial filters and projects the original signal into a new space in order to maximize the differences in variances of two kinds of tasks [4]. The projected signal $\mathbf{S_{csp}(t)}$ is given by:

$$\mathbf{S_{csp}(t)} = \mathbf{W x(t)} \tag{3}$$

where $\mathbf{W} \in \mathbf{R^{C \times C}}$ ($\mathbf{C}$ indicates the channel number) is the constructed spatial filters and $\mathbf{x(t)} \in \mathbf{R^{C \times T}}$ is the original signal ($\mathbf{T}$ indicates the time samples). Then, the CSP features $\mathbf{Fea}$ are designed as:

$$\mathbf{Fea} = \log \frac{var(\mathbf{S_f(t)})}{\sum_{i=1}^{2m} var(\mathbf{S_i(t)})}, \; f = (1 \cdots 2m) \tag{4}$$

where $\mathbf{S_f(t)}$ is the first m and last m rows of $\mathbf{S_{csp}(t)}$.The m was set to be 3 in this paper. These series frequency modulated IMFs decomposed by EMD are averaged in two ways for the CSP feature extraction step (the mean value of IMF1 and IMF2, the mean value of IMF1, IMF2 and IMF3).

E. Hilbert-Huang Transform and PLV Calculation

Hilbert-Huang Transform (HHT) employs the EMD method as a preprocessor in face of the unwrapping problem in Hilbert transform [5]. The instantaneous phase of a given signal $c_i(t)$ is calculated as:

$$\tilde{c_i(t)} = \frac{1}{\pi} p.v \int_{-\infty}^{+\infty} \frac{c_i(\tau)}{t - \tau} d\tau \tag{5}$$

$$\theta_i(t) = \arctan \frac{\tilde{c_i(t)}}{c_i(t)} \tag{6}$$

where $\tilde{c_i(t)}$ is the Hilbert transform of $c_i(t)$ and $p.v$ implies the Cauchy principal value. $\theta_i(t)$ denotes the instantaneous phase.

Given two signal $x_1(t)$ and $x_2(t)$, and $\theta_1(t)$ and $\theta_2(t)$ their corresponding instantaneous phases, the phase difference is defined as $\Delta\theta(t) = \theta_1(t) - \theta_2(t)$. This phase difference is fluctuating and a statistical criterion is employed to quantify the degree of phase locking. Then the PLV is:

$$PLV(t) = |\langle e^{j\Delta\theta(t)} \rangle_t| \tag{7}$$

where $\langle \cdot \rangle_t$ indicates the operator of moving averaged over a time. In the case of two signal are completed synchronized, $\Delta\theta(t)$ is a constant and $PLV(t)$ equals 1. Conversely, if the two signals are unsynchronized, $\Delta\theta(t)$ follows a uniform distribution and $PLV(t)$ equals 0. Here PLV calculation was applied to the IMF2 that contains the μ rhythm. For investigating the PLV between M1 and SMA, six pairs of electrodes were selected, i.e. FCz-CFC3, FCz-C3 and FCz-CPC3 for the left cortex, FCz-CFC4, FCz-C4 and FCz-CPC4 for the right cortex. A time window of 1s is adopted for calculating and the sliding window is 100ms.

For the purpose of mitigating the influence of the volume conduction effect on the PLV calculation, we utilized the idea that from the ERD/ERS calculation [2] and re-calculated the PLV in relation to a 2s reference period during pre-task 2 seconds. It can be expressed as follows:

$$PLV_{ref} = \frac{1}{T}\sum_{r_0}^{r_0+T} PLV(t) \tag{8}$$

$$PLV_r(t) = \frac{PLV(t) - PLV_{ref}}{PLV_{ref}} \times 100\% \tag{9}$$

where PLV_{ref} is the mean PLV of the reference period $[r_0, r_0+T]$ and $PLV_r(t)$ is the re-calculated PLV (see Fig. 3). After that, the $PLV_r(t)$ was re-averaged to constructed a 6 elements feature vector and each element represented a PLV within a time period. Hence, the PLV feature vector can be expressed as:

$$\mathbf{PLV_{C3}} = [plv_1, plv_2 \cdots, plv_6]_{1\times 6} \tag{10}$$

where $\mathbf{PLV_{C3}}$ indicates the PLV feature vector calculated between FCz and C3 electrodes. Next, we constructed the two-dimension PLV features (e.g. FCz-C3 with FCz-C4) in corresponding two electrode pairs. It can be expressed as:

$$\mathbf{PLV_{C3,C4}} = \begin{bmatrix} plv_{1C3} & \cdots & plv_{6C3} \\ plv_{1C4} & \cdots & plv_{6C4} \end{bmatrix}_{2\times 6} \tag{11}$$

where $\mathbf{PLV_{C3,C4}}$ is the constructed feature. The first row of the matrix indicates $\mathbf{PLV_{C3}}$ and the second one is $\mathbf{PLV_{C4}}$. Then, the features were normalized and we obtained 3 two-dimension PLV feature matrixes over all channel pairs. Then we connected these two-dimension PLV feature matrixes and constructed one PLV feature matrix that can be expressed as (due to the limitation of the recorded electrodes, in recorded dataset there are only two pairs of electrodes, FCz-C3 and FCz-C4, the feature matrix was not connected):

$$\mathbf{PLV_{allp}} = \begin{bmatrix} plv_{1CFC3} & \cdots & plv_{1C3} & \cdots & plv_{1CPC3} \\ plv_{1CFC4} & \cdots & plv_{1C4} & \cdots & plv_{1CPC4} \end{bmatrix}_{2\times 18} \tag{12}$$

$$\mathbf{PLV_{allr}} = \begin{bmatrix} plv_{1C3} & \cdots & plv_{6C3} \\ plv_{1C4} & \cdots & plv_{6C4} \end{bmatrix}_{2\times 6} \tag{13}$$

where $\mathbf{PLV_{allp}}$ is the connected two-dimension PLV features for public dataset and $\mathbf{PLV_{allr}}$ for the recorded dataset. Subsequently, we used a linear algebra method to evaluate the feature separability and selected 3 most discriminative two-dimension PLV features from the feature pool:

$$D = \frac{\|\mathbf{f_{left}} - \mathbf{f_{right}}\|^2}{tr(\mathbf{cov_{left}})^2 + tr(\mathbf{cov_{right}})^2} \tag{14}$$

where D reflects the separability of the two-dimension PLV features between two kinds of mental tasks and the higher value indicates more discriminative. $\mathbf{f_{left}}$ and $\mathbf{f_{right}}$ is the mean value of the PLV features in left and right hand task, respectively. $\|\cdot\|$ represents the 2-norm. $\mathbf{cov_{left}}$ and $\mathbf{cov_{right}}$ are the covariance matrixes of the PLV features corresponding to the different tasks. $tr(\cdot)$ means the trace calculation. Finally, we constructed 3 two-dimension PLV features in selected electrode pairs and selected time periods.

F. SFFS Algorithm and Classification

The 3 two-dimension CSP features and 3 two-dimension PLV features were combined and fed into the SFFS feature selection algorithm. 3 two-dimension features were selected and used for the final classification. The linear support vector machines (LSVM) was chosen as the classifier. A 10×10 cross-validation was applied to evaluate the classification performance. A 3s EEG signal segment during the execution period was used for the CSP and PLV feature extraction procedure for both the public and the recorded dataset.

III. Result

A. Classification Result

The classification accuracy of the proposed method on public and recorded dataset was showed in Table I and Table II. CSP_0 means the traditional CSP method. Pha indicates the classification accuracy with only the PLV features. PI_1I_2 and $PI_1I_2I_3$ is the result of the proposed method that utilized the mean of IMF1 and IMF2 or the mean of IMF1, IMF2 and IMF3 in CSP feature extraction step.

As illustrated in Table I, the $PI_1I_2I_3$ led to an improved average performance of 92.97% comparing with the other methods. And a statistically significant difference appeared between $PI_1I_2I_3$ and the traditional CSP method (paired t-test, p = 0.027). The PI_1I_2 failed to increase the average accuracy and it is possible that the IMF3 also conveys the motor imagery intention in subject B but it was omitted by the PI_1I_2 method. As shown in Table II, both the PI_1I_2 and $PI_1I_2I_3$ method lead to an improvement of the classification accuracy and reveal a significant difference (paired t-test, p = 0.045 for PI_1I_2 method; paired t-test, p = 0.044 for $PI_1I_2I_3$ method). The Pha method failed to achieve a high average classification accuracy means only the phase features is insufficient to completely reflect the motor imagery intention, although it may be well discriminates different tasks for some individual subjects (e.g. A in Table I and S1 in Table II).

The high classification accuracy of the $PI_1I_2I_3$ method demonstrates that the proposed feature extraction method fulfills the requirements of the CSP filter and PLV calculation simultaneously. And the combination of the amplitude and the phase information under a uniform feature extraction framework could better reflect brain activities and contribute to enhance the classification accuracy.

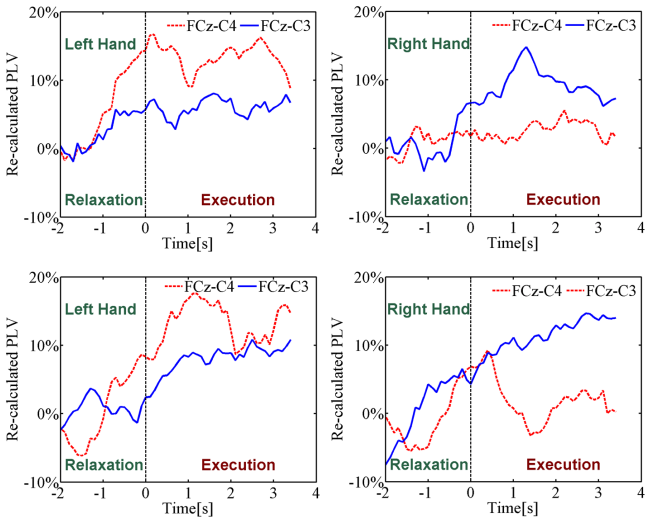

Figure 3. The re-calculated PLV of one subject during two kinds of tasks in public dataset (top row) and one subject of recorded dataset (bottom row)

TABLE I
CLASSIFICALTION ACCURACY (MEAN ± STANDARD DEVIATION IN %) OF THE PUBLICLY AVAILABLE DATASET

Subjects	A	B	C	D	Mean
CSP_0	78.85 ± 2.2	93.56 ± 0.8	96.80 ± 0.9	94.72 ± 0.7	90.98
Pha	84.45 ± 0.6	72.15 ± 1.3	91.70 ± 0.2	84.85 ± 0.7	83.29
PI_1I_2	77.95 ± 2.0	81.05 ± 1.9	98.45 ± 0.8	94.05 ± 0.7	87.88
$PI_1I_2I_3$	82.20 ± 2.5	94.65 ± 1.7	98.85 ± 0.5	96.20 ± 0.9	*92.97**

Statistical significant result is displayed in italic with a superscript asterisk

TABLE II
CLASSIFICALTION ACCURACY (MEAN ± STANDARD DEVIATION IN %) OF THE RECORDED DATASET

Subjects	S1	S2	S3	S4	Mean
CSP_0	70.32 ± 2.2	91.63 ± 0.7	83.50 ± 1.0	78.41 ± 1.2	80.97
Pha	84.46 ± 0.7	75.51 ± 1.0	87.81 ± 1.0	89.23 ± 1.2	84.36
PI_1I_2	84.94 ± 1.9	93.42 ± 1.2	92.12 ± 1.4	88.79 ± 0.8	*89.81**
$PI_1I_2I_3$	83.86 ± 2.5	93.39 ± 0.7	91.36 ± 2.0	90.07 ± 1.6	*89.67**

Statistical significant result is displayed in italic with a superscript asterisk

TABLE III
CLASSIFICALTION ACCURACY (MEAN ± STANDARD DEVIATION IN %) OF THE PUBLICLY AVAILABLE DATASET AND RECORDED DATASET WITHOUT SFFS

Subjects	A	B	C	D	Mean
$PI_1I_2I_3$	79.85 ± 1.5	93.63 ± 1.2	98.65 ± 0.4	95.49 ± 0.9	91.91
Subjects	**S1**	**S2**	**S3**	**S4**	**Mean**
$PI_1I_2I_3$	86.13 ± 1.2	93.23 ± 0.8	85.04 ± 1.3	81.87 ± 1.0	86.56

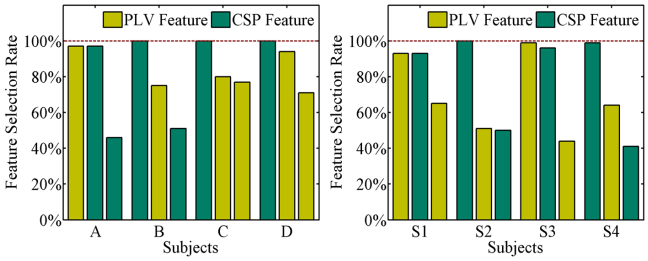

Figure 4. The first three highest feature selection rates in the SFFS procedure for public dateset (left) and recorded dateset (right). The red dashed line indicates the 100 percent selection rate

B. *Classification without SFFS*

As the feature selection procedure is time-consuming, we further evaluated the classification accuracy without the SFFS procedure. First, for each subject we calculated the $PI_1I_2I_3$ feature selected times by the SFFS in the 10×10 cross-validation and divided it by the total classification times as the feature selection rate. As illustrated in Fig. 4 that different types of features (PLV or CSP features) have been selected. Subsequently, we selected those features which reached the top three highest rates as the input to the cross-validation and omitted the SFFS step. As shown in Table III, the classification accuracy is comparable with the result containing the SFFS procedure. It indicates that the information contained in these selected features is relatively stable in each classification time window. Moreover, it implies that the feature selection procedure could be accomplished beforehand and thus it provides the possibility of the online realization of the proposed method.

IV. CONCLUSION

The methodology presented in this paper is a first step to integrate the CSP and PLV features extraction method based on the Empirical Mode Decomposition. The purpose of the method is to fulfill the prerequisite of the CSP filter and the PLV calculation simultaneously, and reflect the brain state during motor imagery form different points of view to contribute to enhance the classification accuracy. It utilizes the filter bank property of the EMD method to satisfy the frequency band requirement in CSP method and employed the IMFs decomposed by EMD as its well-behaved Hilbert transform property to precisely calculate instantaneous phase. It provides a novel strategy of feature extraction procedure for the EEG-based motor imagery BCI system.

Moreover, CSP and PLV generally convey the subject‘s motor intentions in two different ways. CSP can capture the signal amplitude changes and PLV represents the phase dynamics. And these two types of phenomenon could both exist in event related EEG and relatively complemented for each other. Thus combining them together is meaningful, especially when only one type is insufficient to reflect the true brain state and then another could be an alternative.

Finally, this work preliminarily investigates the possibility of the online realization of the proposed method. However, because the EMD algorithm is sensitive to the noise so the predefined IMFs index could be inappropriate for online processing, and future work is required to study how to improve the robustness of the method, especially for online.

ACKNOWLEDGMENT

The authors would like to thank the Berlin BCI group: Berlin Institute of Technology and Fraunhofer FIRST, and Campus Benjamin Franklin of the Charité - University Medicine Berlin, Department of Neurology, Neurophysics Group for providing the data sets in BCI Competition IV.

REFERENCES

[1] J. R. Wolpaw, N. Birbaumer, D. J. McFarland, G. Pfurtscheller, and T. M. Vaughan, "Brain-computer interfaces for communication and control," *Clinical Neurophysiology*, vol. 113, pp. 767-791, Jun 2002.

[2] G. Pfurtscheller and F. H. L. d. Silvab, "Event-related EEG/MEG synchronization and desynchronization: basic principles," *Clinical Neurophysiology*, 1999.

[3] E. Gysels and P. Celka, "Phase synchronization for the recognition of mental tasks in a brain-computer interface," *Neural Systems and Rehabilitation Engineering, IEEE Transactions on*, vol. 12, pp. 406-415, 2004.

[4] G. Pfurtscheller and C. Neuper, "Motor imagery and direct brain-computer communication," *Proceedings of the IEEE*, vol. 89, pp. 1123-1134, 2001..

[5] N. E. Huang, Z. Shen, S. R. Long, M. C. Wu, H. H. Shih, Q. Zheng, *et al.*, "The empirical mode decomposition and the Hilbert spectrum for nonlinear and non-stationary time series analysis," *Proceedings of the Royal Society of London. Series A: Mathematical, Physical and Engineering Sciences,* vol. 454, p. 903, 1998.

[6] P. Flandrin, G. Rilling, and P. Goncalves, "Empirical mode decomposition as a filter bank," *Signal Processing Letters, IEEE,* vol. 11, pp. 112-114, 2004.

[7] P. Pudil, J. Novovicová, and J. Kittler, "Floating search methods in feature selection," *Pattern Recognition Letters,* vol. 15, pp. 1119-1125, 1994.

[8] H. Sanqing, M. Stead, and G. A. Worrell, "Automatic Identification and Removal of Scalp Reference Signal for Intracranial EEGs Based on Independent Component Analysis," *Biomedical Engineering, IEEE Transactions on*, vol. 54, pp. 1560-1572, 2007.

[9] R. Ranta and N. Madhu, "Reference Estimation in EEG: Analysis of Equivalent Approaches," *Signal Processing Letters, IEEE*, vol. 19, pp. 12-15, 2012.